

# Tube-based Internal Model Control and its Application to Temperature Control in Buildings<sup>\*</sup>

M. Löhning<sup>\*</sup> S. Reimann<sup>\*</sup> P. Kotman<sup>\*</sup>

<sup>\*</sup> Robert Bosch GmbH, Stuttgart, Germany  
(e-mail: {martin.loehning, sven.reimann,  
philipp.kotman}@de.bosch.com).

---

## Abstract:

Indoor climate control is a central topic in modern buildings. Especially office spaces have to provide a high comfort for the occupants while at the same time the building operation should require as little energy as possible. Moreover, an upcoming topic in building automation is a fast reaction to user feedback. The traditional design of a room temperature controller focuses solely on a good rejection of input disturbances such as variations of occupancy and solar radiation. Since the transfer functions of the user feedback and the input disturbances to the room temperature differ, a fast reaction to user feedback requires rethinking the design of a room temperature controller. Altogether, there is a desire to use modern controllers for room temperature control.

To ensure indoor comfort, the room temperature has to be kept within a certain interval. In this paper, the internal model control method is extended such that the controlled variable is kept in the tube defined by this temperature interval. The main idea is to compute an admissible tube for the planned trajectory. This results in an interval for the control input, which provides a degree of freedom. This is used to minimize the energy consumption. For the implementation in reality, the proposed controller is discretized in time. To ensure a good disturbance attenuation, the controller is combined with a Kalman Filter.

The closed-loop behavior of the developed controller is validated in a real building and compared with a state-of-the-art controller.

*Keywords:* Internal Model Control, Bilinear System, Control of Constrained Systems, Building Automation, Energy Efficiency, Energy and Distribution Management Systems

---

## 1. INTRODUCTION

Indoor climate control is a central topic in modern buildings. Especially office spaces are supposed to be operated in a way such that a high comfort of the occupants is guaranteed. However, HVAC systems account for 20% of the world energy consumption (Pérez-Lombard et al., 2008; Sturzenegger et al., 2016). Consequently, there is an economical and ecological need to reduce the energy consumption of buildings. These goals are contradictory, as an improved indoor comfort often comes with an increased energy consumption. Fortunately, there are degrees of freedom in the building operation that ensure a good indoor comfort while reducing the energy consumption. For example, ensuring indoor comfort is often modeled as keeping the room temperature within a certain interval (DIN EN 15251:2012-12, 2012; ASHRAE, Inc., 2013). Within this interval, the controller can choose the room temperature with the minimum energy consumption.

Traditionally, a room temperature controller is designed for a good rejection of changes in the internal loads like

---

<sup>\*</sup> The authors gratefully acknowledge the financial support of the “FlexControl” project funded by the German Federal Ministry of Economics and Energy (project code: 03ET1359E).

changing solar radiation or occupancy. These changes of the internal load can be modeled as an unknown input disturbance. Furthermore, an upcoming topic in building automation is the reaction to user feedback (Li et al., 2017). Unfortunately, a good attenuation of input disturbances does not guarantee a good response to user feedback. Altogether, there is a requirement to use advanced control design methods for room temperature control.

An overview of controllers for HVAC systems is given in (Afram and Janabi-Sharifi, 2014). According to Afram and Janabi-Sharifi (2014) the control of HVAC systems is challenging due to nonlinear dynamics, time-varying set-points and disturbances, poor data due to low resolution of analog to digital converters, sampling rates, and accuracy of sensors. The state-of-the-art in room temperature control are PID controllers (Bai et al., 2008). Tuning the PID controller can be time consuming and expensive (Bai et al., 2008). Hence, most PID controllers are operated with a default set of parameters.

An alternative which implicitly adapts the control parameters to the building and zone at hand are model-based control approaches. One approach which is often found in the literature of building automation is model predictive

control (Afram and Janabi-Sharifi, 2014; Sturzenegger et al., 2016; Oldewurtel et al., 2010). This approach requires, in general, the online numerical solution of an open-loop optimal control problem, which reduces its acceptance in the field of building automation. Another method is internal model control (IMC) which is known for its applicability to (flat) nonlinear systems, robustness, offset free tracking, and easy tuning (Garcia and Morari, 1982). Hence, the IMC can tackle the challenges mentioned in the last paragraph and is a promising control approach. The IMC has already been used in building automation for the tuning of PID controllers (Fardadi et al., 2005) and lighting control (Kandasamy et al., 2018). However, like most control methods, the IMC is used for tracking a reference signal.

The main contribution of this paper is the extension of the IMC method such that the controlled variable is kept in a tube defined by lower and upper bounds of the controlled variable, i.e., the room temperature for the considered application. Furthermore, controlling the temperature within this tube provides a degree of freedom, which is used to minimize the energy consumption. Instead of computing a reference for tracking, the proposed controller directly computes the energy optimal internal state. For the implementation in reality, the proposed controller is discretized in time. To ensure a good disturbance attenuation, the controller is combined with a Kalman Filter, which estimates the disturbance. Another contribution is the validation of the developed controller in a real building and the comparison with a state-of-the-art PI controller.

In Section 2 the problem setup of temperature control in buildings is described. The proposed IMC approach for tube control is developed in Section 3. Afterwards, the application to the real building including the comparison with the state-of-the-art PI controller is presented in Section 4. Finally, the paper is concluded in Section 5.

## 2. PROBLEM SETUP

In this paper, ensuring a high indoor comfort is translated into keeping the room temperature within a defined comfort interval. Besides a good disturbance attenuation, the controller should achieve a fast reaction to changes of this comfort interval to allow user feedback. If there are degrees of freedom, e.g. redundancies in the actuation variables or by considering a comfort interval instead of a set-point, the controller should furthermore reduce the energy consumption.

The considered HVAC configuration consist of one or more central *air handling units* (AHUs) and one *variable air volume* (VAV) unit for each controlled zone. The AHUs provide a supply air with a predefined temperature. The VAV units feature a flap which allows to change the air mass flow into the zone. For the model-based zone control, it is assumed that the air is ideally mixed within each zone with respect to the temperature. Cross-couplings between the zones are considered as disturbances.

A controller is designed for each zone individually and not for the complete building. The thermal behavior of the zone is modeled as a bilinear SISO system; see Section 4.1 for further details on the modeling of the zone. The control

task is to keep the output signal, which corresponds to the zone temperature, within a desired interval (*tube*) given by  $[y^{lb}, y^{ub}]$ . The tube can be adapted by the user. The input signal  $u$  which corresponds to the air mass flow, is subject to constraints, i.e.  $u \in [u^{min}, u^{max}]$ . The constraints are given by physical limits and/or to have a minimal air exchange.

The bilinear model  $\Sigma$  of one zone has the form

$$\Sigma : \quad \frac{dx}{dt} = axu + bu + c\hat{d} \quad (1a)$$

$$y = x \quad (1b)$$

with the model parameters  $a \neq 0, b, c \in \mathbb{R}$ . The flat output  $y \in \mathbb{R}$  equals the state  $x \in \mathbb{R}$  and the variable  $\hat{d} \in \mathbb{R}$  corresponds to the estimation of a disturbance. The disturbance is assumed to be known for the control design in Section 3. This assumption is dropped in Section 4.2. For ease of presentation, the derivations are restricted to such systems. It is worth emphasizing that the approach can be extended to more general system classes.

## 3. TUBE-BASED IMC

This section introduces a novel tube-based IMC approach, which addresses the problem of controlling the output to a desired interval and reducing the energy demand if the output is already in this interval. Before introducing the method in Section 3.3, the flatness-based IMC for set-point tracking is revisited in Section 3.1. In Section 3.2 the focus is on the discrete-time implementation which is relevant for the validation on the test bench.

### 3.1 IMC for set-point tracking

Internal model control is a model-based control approach which ensures important properties of a feedback controller such as disturbance attenuation and offset-free tracking.

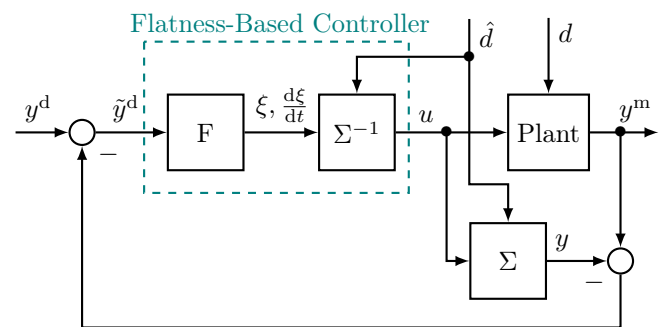


Fig. 1. Flatness-based IMC structure for a first order system

Figure 1 shows the IMC structure for tracking the desired set-point  $y^d$  with the plant, a flatness-based controller and a plant model  $\Sigma$ . A disturbance  $d$  acts on the plant. The flatness-based controller contains a filter  $F$  for determining a desired trajectory given by  $\xi$  and  $d\xi/dt$ , a flatness-based inverse  $\Sigma^{-1}$  of the plant model  $\Sigma$  for determining the control input  $u$  based on the desired trajectory and an estimate  $\hat{d}$  of the disturbance  $d$ . Since only systems of order one are considered, the trajectory is defined by the internal state  $\xi$  and its first derivative  $d\xi/dt$  w.r.t. time. It is

determined using a filter, which is given by the first-order lag element

$$F : \frac{d\xi}{dt} = \frac{1}{\tau} (-\xi + \tilde{y}^d)$$

as well as a saturation of the derivative  $d\xi/dt$  such that the trajectory is realizable with  $u \in [u^{\min}, u^{\max}]$  (Schwarzmann et al., 2006). The time constant  $\tau > 0$  is a design parameter, which defines how fast the closed-loop tracks the desired output  $y^d$  if the input is not saturated. The difference between the measured plant output  $y^m$  and the model output  $y$  is used as the feedback signal. From the control structure with the inverse model and the model follows that  $y = \xi$ . Hence, the filter can also be represented by

$$F : \frac{d\xi}{dt} = \frac{1}{\tau} (y^d - y^m). \quad (2)$$

The mode of operation can be summarized as follows: In case of a perfect model, knowledge of the initial state, and perfect disturbance knowledge, i.e.  $\hat{d} = d$ , the feedback is  $y^m - y = 0$  such that the internal model controller acts as a feedforward controller. In case of disturbances or model uncertainties the feedback structure changes the original reference signal  $y^d$  for the flatness-based controller into a new reference signal  $\tilde{y}^d = y^d - (y^m - y)$ . For more details see (Garcia and Morari, 1982; Schwarzmann et al., 2006) and the references therein.

### 3.2 Discrete-Time Implementation

For the implementation in real buildings, a discrete-time formulation of the IMC is required. The discrete-time IMC is then extended for tube control in the following section.

The plant model (1) and the filter (2) are discretized with the implicit Euler method (Butcher, 2016) and the sample time  $h = t_k - t_{k-1}$ . The continuous-time bilinear model (1) and linear filter (2) are thus transformed to the explicit discrete-time plant model

$$\Sigma : \begin{aligned} x_k &= f(x_{k-1}, u_k, \hat{d}_k) \\ y_k &= x_k \end{aligned}$$

with

$$f(x_{k-1}, u_k, \hat{d}_k) = \frac{x_{k-1} + h(bu_k + c\hat{d}_k)}{1 - ha u_k} \quad (3)$$

and the discrete-time filter equation

$$F : \xi_k^d = \xi_{k-1} + \frac{h}{\tau} (y_k^d - y_k^m). \quad (4)$$

In the following it is assumed that  $ha u_k \neq 1$  for all  $u_k \in [u^{\min}, u^{\max}]$  so that  $f(x_{k-1}, u_k, \hat{d}_k)$  is well defined. For the room temperature control this assumption is satisfied since  $ha < 0$  and  $u_k \geq u^{\min} > 0$  at all times.

The filter state  $\xi_k^d$  needs to be limited such that the trajectory is realizable with  $u \in [u^{\min}, u^{\max}]$  (Kotman, 2018). Since the function  $f(x_{k-1}, u_k, \hat{d}_k)$  is monotonous in  $u_k$  for all  $u_k \in [u^{\min}, u^{\max}]$ , it suffices to saturate  $\xi_k^d$  to the values obtained at the limits of the input

$$\xi_k^{\min} = \min(f(\xi_{k-1}, u^{\min}, \hat{d}_k), f(\xi_{k-1}, u^{\max}, \hat{d}_k)) \quad (5a)$$

$$\xi_k^{\max} = \max(f(\xi_{k-1}, u^{\min}, \hat{d}_k), f(\xi_{k-1}, u^{\max}, \hat{d}_k)). \quad (5b)$$

With the saturation function

$$\text{sat}(z, z^{\min}, z^{\max}) = \begin{cases} z^{\min} & \text{if } z < z^{\min} \\ z^{\max} & \text{if } z > z^{\max} \\ z & \text{otherwise} \end{cases}, \quad (6)$$

the saturated internal state is written as

$$\xi_k = \text{sat}(\xi_k^d, \xi_k^{\min}, \xi_k^{\max}).$$

In the following, the inversion  $\Sigma^{-1}$  of the model  $\Sigma$  is derived which determines the control input. If  $\xi_k = -b/a$ , then the equation

$$\xi_k = f(\xi_{k-1}, u_k, \hat{d}_k) \quad (7)$$

cannot be solved for  $u_k$ . If, furthermore,  $\xi_{k-1} + hc\hat{d}_k = -b/a$ , then (7) is fulfilled for all  $u_k \in [u^{\min}, u^{\max}]$  and one possible choice is to use the input with the lowest energy consumption. The case  $\xi_k = -b/a$  and  $\xi_{k-1} + hc\hat{d}_k \neq -b/a$ , in which (7) is not fulfilled, cannot occur. To see this, note that  $f(\xi_{k-1}, u_k, \hat{d}_k) = -b/a$  if and only if  $\xi_{k-1} + hc\hat{d}_k = -b/a$ . Altogether, the input is defined by

$$u_k = f^{\text{inv}}(z, \xi_{k-1}, \hat{d}_k) = \begin{cases} \frac{z - \xi_{k-1} - hc\hat{d}_k}{h(a z + b)} & \text{if } z \neq -\frac{b}{a} \\ u^{\min} & \text{otherwise} \end{cases}. \quad (8)$$

The discrete-time implementation of the IMC with input saturation is stated in Algorithm 1.

---

**Algorithm 1** Discrete-time implementation of the IMC at the time instant  $t = t_k$

---

**Step 1:** Initialization

$$\xi_{k-1}, y_k^d, y_k^m, \hat{d}_k$$

**Step 2:** Trajectory planning with filter F

$$\xi_k^d = \xi_{k-1} + \frac{h}{\tau} (y_k^d - y_k^m)$$

$$\xi_k^{\min} = \min(f(\xi_{k-1}, u^{\min}, \hat{d}_k), f(\xi_{k-1}, u^{\max}, \hat{d}_k))$$

$$\xi_k^{\max} = \max(f(\xi_{k-1}, u^{\min}, \hat{d}_k), f(\xi_{k-1}, u^{\max}, \hat{d}_k))$$

$$\xi_k = \text{sat}(\xi_k^d, \xi_k^{\min}, \xi_k^{\max})$$

**Step 3:** Control input determination based on  $\Sigma^{-1}$

$$u_k = f^{\text{inv}}(\xi_k, \xi_{k-1}, \hat{d}_k)$$


---

### 3.3 Discrete-Time Tube-Based IMC

In the following, the concept of internal model control is extended to tube control. In short, the idea is to compute two target trajectories  $\xi_k^{\text{lb}}$  and  $\xi_k^{\text{ub}}$  for tracking the lower bound  $y_k^{\text{lb}}$  and upper bound  $y_k^{\text{ub}}$  of the tube, respectively. Then, the two target trajectories can be used to compute a lower bound  $u_k^{\text{lb}}$  and upper bound  $u_k^{\text{ub}}$  for the input such that the output converges to a value within the boundaries  $y_k^{\text{lb}}, y_k^{\text{ub}}$ . Finally, the input is selected such that the minimum energy consumption is achieved.

The two target trajectories are determined similar to the discretized filter (4) by

$$\xi_k^{\text{lb}} = \xi_{k-1} + \frac{h}{\tau} (y_k^{\text{lb}} - y_k^m), \quad \xi_k^{\text{ub}} = \xi_{k-1} + \frac{h}{\tau} (y_k^{\text{ub}} - y_k^m).$$

The input constraints can be taken into account using the limits (5) and saturation function (6). Based on the saturated target trajectories, an interval for the control input  $[u_k^{\text{lb}}, u_k^{\text{ub}}]$  is determined using (8). If the interval of the input is proper, there exists a degree of freedom, which is used to reduce the energy consumption. Depending on the chosen input  $u_k \in [u_k^{\text{lb}}, u_k^{\text{ub}}]$  the realized trajectory of the filter is computed by (7).

Algorithm 2 summarizes the procedure for tube control using IMC. In contrast to Algorithm 1, lower and upper bounds for the target trajectory are computed instead of the desired target trajectory. With the input saturation, this results in an interval for the target trajectory. The realized target trajectory is implicitly defined in Step 3 by choosing the input such that the energy effort is minimized.

**Algorithm 2** Discrete-time implementation of Tube Control using IMC at the time step  $t = t_k$

**Step 1:** Initialization

$$\xi_{k-1}, y_k^{\text{lb}}, y_k^{\text{ub}}, y_k^{\text{m}}, \hat{d}_k$$

**Step 2:** Trajectory planning with filter F

**a:** Trajectory interval w.r.t. desired tube

$$\xi_k^{\text{lb}} = \xi_{k-1} + \frac{h}{\tau}(y_k^{\text{lb}} - y_k^{\text{m}})$$

$$\xi_k^{\text{ub}} = \xi_{k-1} + \frac{h}{\tau}(y_k^{\text{ub}} - y_k^{\text{m}})$$

**b:** Mapping constraints of input to internal state

$$\xi_k^{\text{min}} = \min(f(\xi_{k-1}, u^{\text{min}}, \hat{d}_k), f(\xi_{k-1}, u^{\text{max}}, \hat{d}_k))$$

$$\xi_k^{\text{max}} = \max(f(\xi_{k-1}, u^{\text{min}}, \hat{d}_k), f(\xi_{k-1}, u^{\text{max}}, \hat{d}_k))$$

**c:** Saturation of trajectory interval w.r.t. constraints

$$\xi_k^{\text{b1}} = \text{sat}(\xi_k^{\text{lb}}, \xi_k^{\text{min}}, \xi_k^{\text{max}})$$

$$\xi_k^{\text{b2}} = \text{sat}(\xi_k^{\text{ub}}, \xi_k^{\text{min}}, \xi_k^{\text{max}})$$

**Step 3:** Control input determination based on  $\Sigma^{-1}$

$$u_k^{\text{lb}} = \min(f^{\text{inv}}(\xi_k^{\text{b1}}, \xi_{k-1}, \hat{d}_k), f^{\text{inv}}(\xi_k^{\text{b2}}, \xi_{k-1}, \hat{d}_k))$$

$$u_k^{\text{ub}} = \max(f^{\text{inv}}(\xi_k^{\text{b1}}, \xi_{k-1}, \hat{d}_k), f^{\text{inv}}(\xi_k^{\text{b2}}, \xi_{k-1}, \hat{d}_k))$$

Select  $u_k \in [u_k^{\text{lb}}, u_k^{\text{ub}}]$  that results in the minimum energy consumption.

**Step 4:** Storage of internal state

$$\xi_k = f(\xi_{k-1}, u_k, \hat{d}_k)$$

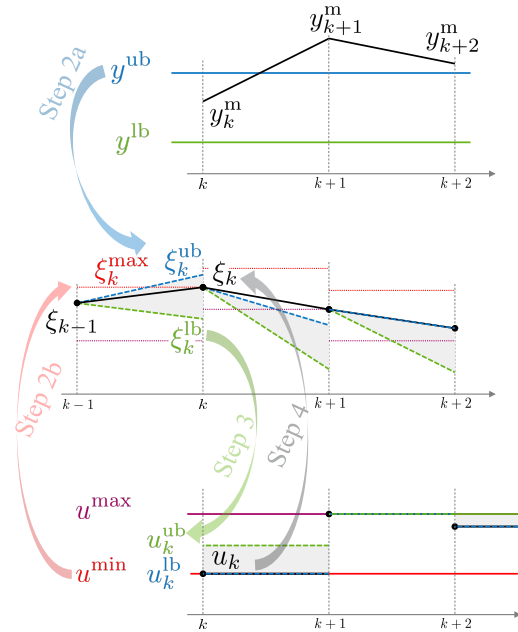


Fig. 2. Visualization of Tube Control using IMC

#### 4. APPLICATION TO TEMPERATURE CONTROL IN BUILDINGS

Figure 2 visualizes the concept and emphasizes the different steps of Algorithm 2 for an exemplified trajectory. The example is based on the application considered in Section 4, where for the usual operation conditions  $df/du < 0$  holds. Hence, Step 2b-3 simplifies to

$$\xi_k^{\text{min}} = f(\xi_{k-1}, u^{\text{max}}, \hat{d}_k)$$

$$\xi_k^{\text{max}} = f(\xi_{k-1}, u^{\text{min}}, \hat{d}_k)$$

$$u_k^{\text{lb}} = f^{\text{inv}}(\text{sat}(\xi_k^{\text{ub}}, \xi_k^{\text{min}}, \xi_k^{\text{max}}), \xi_{k-1}, \hat{d}_k)$$

$$u_k^{\text{ub}} = f^{\text{inv}}(\text{sat}(\xi_k^{\text{lb}}, \xi_k^{\text{min}}, \xi_k^{\text{max}}), \xi_{k-1}, \hat{d}_k).$$

Furthermore, the energy effort is minimized by choosing the minimum control input.

In Step 2 at the time instant  $k$  the interval of the target trajectory given by  $\xi_k^{\text{lb}}$  and  $\xi_k^{\text{ub}}$  is determined, whereas  $\xi_k^{\text{ub}}$  is saturated to  $\xi_k^{\text{max}}$  due to the input constraints. Therefore, the control input  $u_k^{\text{lb}}$  corresponding to the saturated  $\xi_k^{\text{ub}}$  is equal to the minimum control input, i.e.  $u_k^{\text{lb}} = u^{\text{min}}$ . In order to reduce the energy effort  $u_k = u_k^{\text{lb}} = u^{\text{min}}$  is selected as control input in Step 3. In Step 4, the internal state  $\xi_k$  is updated based on the selected control input  $u_k$ . Due to an increasing output  $y_{k+1}^{\text{m}}$ , which may be caused by a disturbance for instance, both target trajectories  $\xi_{k+1}^{\text{lb}}$  and  $\xi_{k+1}^{\text{ub}}$  are below the maximal internal state realizable with the input constraints. Hence, the internal state is saturated to  $\xi_{k+1}^{\text{min}}$ . Therefore, the control input is equal to  $u_{k+1} = u^{\text{max}}$ . Due to a decreasing output, the control input can be reduced to  $u_{k+2} < u^{\text{max}}$  at the time instant  $k+2$ .

The introduced tube-based IMC is implemented for the temperature control on an SPS. In an office building, the temperature of all zones of one floor is controlled using *variable air volumes* (VAVs) units. The zones are meeting rooms or sections of an open plan office. The transmission of the measurement and actuator signals is realized via BACnet. Before showing the implementation results in Section 4.3, the application of the control algorithm on the temperature control problem is discussed in Sections 4.1 and 4.2.

##### 4.1 Problem setup

The dynamic model describing the thermal behavior of a zone is given by

$$\frac{d\vartheta_{\text{zone}}}{dt} = C_{\text{zone}}^{-1} (\dot{m}_{\text{vent}} c_{\text{air}} (\vartheta_{\text{air, supply}} - \vartheta_{\text{zone}}) + \dot{Q}_{\text{dist}}) \quad (9)$$

where the zone air temperature  $\vartheta_{\text{zone}}$  is the output signal and the fresh air mass flow  $\dot{m}_{\text{vent}}$  is the input signal. The supply air temperature  $\vartheta_{\text{air, supply}}$  is assumed to be measurable, and the heat capacity of the zone  $C_{\text{zone}}$  and the specific heat of air  $c_{\text{air}}$  are model parameters. The unknown disturbance signal  $\dot{Q}_{\text{dist}}$  summarizes disturbances such as internal loads by occupants or technical devices, solar radiation or heat exchange between zones. Further details on building modeling can, e.g., be found in (Massa Gray, 2017).

Based on the dynamic model (9), Algorithm 2 can be applied with

$$a = -C_{\text{zone}}^{-1} c_{\text{air}}, \quad b = C_{\text{zone}}^{-1} c_{\text{air}} \vartheta_{\text{air, supply}}, \quad c = C_{\text{zone}}^{-1}$$

where  $y_k^{\text{lb}} = \vartheta_{\text{zone}}^{\text{lb}}$  and  $y_k^{\text{ub}} = \vartheta_{\text{zone}}^{\text{ub}}$  define the comfort interval of the temperature which can optionally be adapted by user feedback. The maximum control input  $u^{\text{max}} = \dot{m}_{\text{vent}}^{\text{max}}$  is given by the limits of the HVAC system. The minimum control input  $u^{\text{min}} = \dot{m}_{\text{vent}}^{\text{min}}$  is usually chosen

larger than zero in order to always guarantee a minimum air exchange. At Step 3 of Algorithm 2, the minimum energy consumption is achieved by selecting the minimum air mass flow.

For testing the developed controller, only the cooling case is considered, i.e. the supply air temperature  $\vartheta_{\text{air,supply}}$  from the air handling unit (AHU) is smaller than the zone air temperature.

#### 4.2 Combination of Tube-based IMC with Disturbance Estimation

So far it is assumed that an estimation of the disturbance  $\hat{d}$  is available. This estimation can, .e.g., be determined using a Kalman Filter (Gelb, 1974). The Kalman Filter can additionally be applied to filter the measured zone temperature, which is quantized in the considered building.

If there is no knowledge about the disturbance model, a common approach is to assume a constant disturbance signal. Extending the zone model yields the augmented state space model

$$\begin{aligned} \frac{d\vartheta_{\text{zone}}}{dt} &= C_{\text{zone}}^{-1} \left( \dot{m}_{\text{vent}} c_{\text{air}} (\vartheta_{\text{air,supply}} - \vartheta_{\text{zone}}) + \dot{Q}_{\text{dist}} \right) \\ \frac{d\dot{Q}_{\text{dist}}}{dt} &= 0. \end{aligned}$$

Due to the bilinearity of the model, an extended Kalman Filter is applied, which estimates the zone temperature  $\vartheta_{\text{zone}}$  and disturbance  $\dot{Q}_{\text{dist}}$ . Those estimates are used as  $y_k^m$  and  $\hat{d}$  for the initialization in Step 1 of Algorithm 2.

#### 4.3 Control Performance

The introduced tube-based internal model control combined with the disturbance estimation is implemented in all zones of one floor of an office building in Renningen, Germany. Detailed analyses for the temperature control are made in a meeting room, which is selected such that the unknown disturbances are minimized: the room has no windows, is located in the middle of the floor to reduce the effect of the ambient air temperature, and the door was closed all the time. A heat source allows generating definable thermal loads such that comparable conditions for several days can be realized. In this setup, the proposed model-based controller is compared with a state-of-the-art PI controller.

The state-of-the-art controller consists of two PI controllers, one for cooling if the zone temperature is above the upper bound and one for heating if the zone temperature is below the lower bound. Depending on the supply air temperature and the output of both PI controllers, the PI controller for the upper or lower bound is activated. The structure of the PI controller is depicted in Figure 3.

The comparison of the IMC with the PI controller is made with respect to disturbance attenuation and the reaction on user feedback. In this context, user feedback means the adaptation of the comfort interval by the user.

Figure 4 compares the reaction to user feedback. Before 7 a.m., the zone temperature is within the comfort interval, such that there is no comfort violation. At 7 a.m. there is a user feedback such that the upper bound of the comfort interval is reduced. The new upper bound is selected

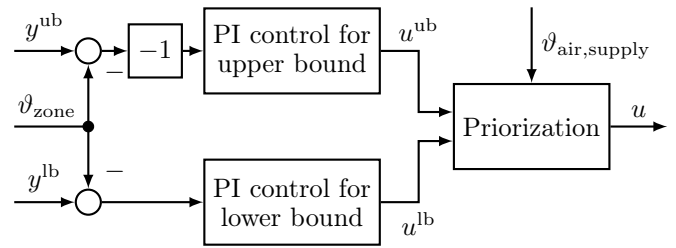


Fig. 3. Structure of the PI controller

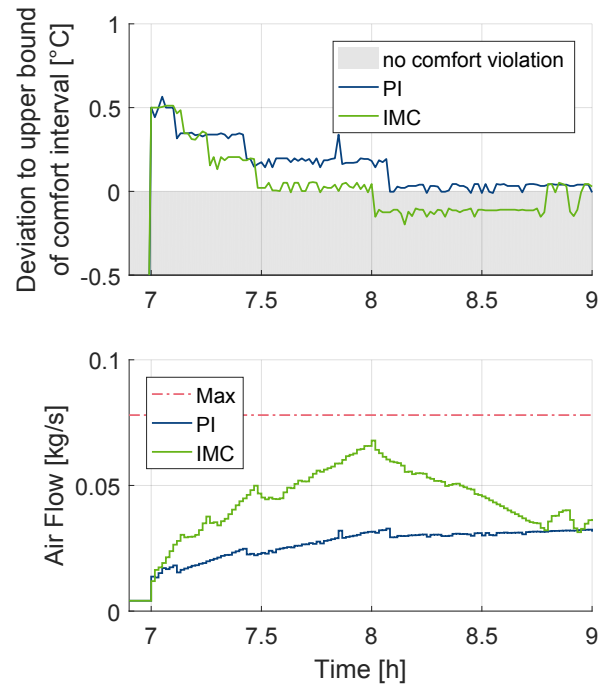


Fig. 4. Comparison with respect to user feedback

0.5 K below the measured temperature at 7 a.m.. For both controllers, the air flow with a supply air temperature of about 17 °C is at the minimum air flow  $\dot{m}_{\text{vent}}^{\text{min}}$  before 7 a.m.. At 7 a.m. the deviation to the upper bound of the comfort interval increases to 0.5 K, such that there is a comfort violation. Figure 4 clearly shows that the two controllers react differently to the user feedback. Applying the IMC, the zone temperature converges to the new limit of the comfort interval within half an hour, whereas when using the PI controller, more than one hour is required. This can be explained by the faster increase of the air mass flow. The convergence rate of the IMC can also be easily adapted using the time constant  $\tau$ . Achieving a performance with the PI controller similar to the IMC could possibly be achieved by a reparametrization of the PI controller. But a parametrization of the PI controller to the building at hand is in general not done due to the large effort.

For the disturbance attenuation shown in Figure 5, a heat generation device is turned on at 8 a.m., creating a load of about 250 W. The IMC shows a slightly better disturbance attenuation than the PI controller when the temperature reaches the upper limit of the comfort interval  $\vartheta_{\text{zone}}^{\text{ub}} = 24^\circ\text{C}$ . The PI controller causes an overshooting of the zone air temperature, which can be avoided using the

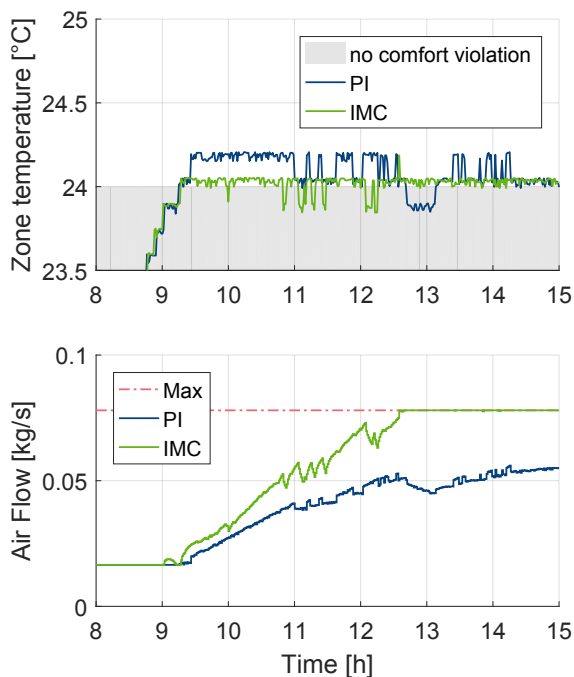


Fig. 5. Comparison with respect to disturbance attenuation IMC. This can be explained based on the structure of the control approaches. The PI controller only increases the air mass flow when the upper limit of the comfort interval is exceeded, whereas the IMC already increases the air mass flow when the upper limit is approached. Additionally, the IMC shows a faster increase of the air mass flow, leading to a better disturbance attenuation.

## 5. CONCLUSION

The paper presents tube-based IMC, which extends IMC to track a desired interval – and not a set-point – of the controlled variable. Keeping the controlled variable within an interval provides a degree of freedom, which can be used to minimize, for example, the energy consumption. For the considered bilinear SISO systems with input constraints, a computationally efficient analytic algorithm achieves the minimization of the energy of the input variable.

Furthermore, the proposed controller is applied to temperature control in buildings. For the implementation in reality, the proposed controlled is discretized in time. To ensure a good disturbance attenuation, the controller is combined with a Kalman Filter. Essential insights have been gained by the comparison of the IMC with a state-of-the-art PI zone temperature controller in a real building. Using an artificial, and hence reproducible, disturbance in a closed meeting room allowed a meaningful comparison of the closed-loop performance of both controllers. The main advantage of the IMC is the significantly faster reaction to set-point changes, which makes it well suited for applications in which a fast reaction to user feedback is desired.

Future work investigates the extension to a combined temperature and CO<sub>2</sub> control or multiple inputs, i.e., HVAC systems with radiators or variable air volume fan-powered terminal units as well as the online adaptation of model and design parameters.

## REFERENCES

- Afram, A. and Janabi-Sharifi, F. (2014). Theory and applications of HVAC control systems – a review of model predictive control (MPC). *Building and Environment*, 72, 343–355.
- ASHRAE, Inc. (2013). ASHRAE standard 55: Thermal environmental conditions for human occupancy.
- Bai, J., Wang, S., and Zhang, X. (2008). Development of an adaptive smith predictor-based self-tuning PI controller for an HVAC system in a test room. *Energy and Buildings*, 40(12), 2244–2252.
- Butcher, J.C. (2016). *Numerical methods for ordinary differential equations*. John Wiley & Sons.
- DIN EN 15251:2012-12 (2012). Eingangparameter für das Raumklima zur Auslegung und Bewertung der Energieeffizienz von Gebäuden - Raumluftqualität, Temperatur, Licht und Akustik. Deutsches Institut für Normung e.V. Deutsche Fassung EN 15251.
- Fardadi, M., Ghafari, A.S., and Hannani, S. (2005). IMC based, robust PID controller tuning for SUT building energy management system. In *Proceedings of the 24th IASTED International Conference on Modelling, Identification, and Control*, 58–63.
- Garcia, C.E. and Morari, M. (1982). Internal model control. A unifying review and some new results. *Industrial & Engineering Chemistry Process Design and Development*, 21(2), 308–323.
- Gelb, A. (1974). *Applied Optimal Estimation*. MA: MIT Press.
- Kandasamy, N.K., Karunagaran, G., Spanos, C., Tseng, K.J., and Soong, B.H. (2018). Smart lighting system using ANN-IMC for personalized lighting control and daylight harvesting. *Building and Environment*, 139, 170–180.
- Kotman, P. (2018). *Modeling and control of diesel engine air systems*. Ph.D. thesis, TU Vienna.
- Li, D., Menassa, C.C., and Kamat, V.R. (2017). A personalized HVAC control smartphone application framework for improved human health and well-being. In *Computing in Civil Engineering 2017*, 82–90.
- Massa Gray, F. (2017). *Gaussian Process Building Model and their Application in Model Predictive Control*. Ph.D. thesis, University of Stuttgart.
- Oldewurtel, F., Parisio, A., Jones, C.N., Morari, M., Gyalistras, D., Gwerder, M., Stauch, V., Lehmann, B., and Wirth, K. (2010). Energy efficient building climate control using stochastic model predictive control and weather predictions. In *Proceedings of the 2010 American Control Conference*, 5100–5105.
- Pérez-Lombard, L., Ortiz, J., and Pout, C. (2008). A review on buildings energy consumption information. *Energy and Buildings*, 40(3), 394–398.
- Schwarzmann, D., Nitsche, R., Lunze, J., and Schanz, A. (2006). Pressure control of a two-stage turbocharged diesel engine using a novel nonlinear IMC approach. In *Proceedings of the 2006 IEEE International Conference on Control Applications*.
- Sturzenegger, D., Gyalistras, D., Morari, M., and Smith, R.S. (2016). Model predictive climate control of a Swiss office building: Implementation, results, and cost-benefit analysis. *IEEE Transactions on Control Systems Technology*, 24(1), 1–12.